

Temporal Interaction between Single Spikes and Complex Spike Bursts in Hippocampal Pyramidal Cells

Kenneth D. Harris,² Hajime Hirase,²
Xavier Leinekugel,² Darrell A. Henze,
and György Buzsáki¹

Center for Molecular and Behavioral Neuroscience
Rutgers, The State University of New Jersey
Newark, New Jersey 07102

Summary

Cortical pyramidal cells fire single spikes and complex spike bursts. However, neither the conditions necessary for triggering complex spikes, nor their computational function are well understood. CA1 pyramidal cell burst activity was examined in behaving rats. The fraction of bursts was not reliably higher in place field centers, but rather in places where discharge frequency was 6–7 Hz. Burst probability was lower and bursts were shorter after recent spiking activity than after prolonged periods of silence (100 ms–1 s). Burst initiation probability and burst length were correlated with extracellular spike amplitude and with intracellular action potential rising slope. We suggest that bursts may function as “conditional synchrony detectors,” signaling strong afferent synchrony after neuronal silence, and that single spikes triggered by a weak input may suppress bursts evoked by a subsequent strong input.

Introduction

Fast series of action potentials, typically referred to as “bursts,” are observed in various neuronal types in the central nervous system (Connors et al., 1982; Gray and McCormick, 1996; Kandel and Spencer, 1961; Llinas and Jahnsen, 1982; Thach, 1968). In the hippocampus, pyramidal cells exhibit bursts of 2–6 spikes of decreasing extracellular amplitude at short (≤ 6 ms) intervals (Ranck, 1973). Two general functions have been attributed to bursts. First, the “downstream” effect of a burst is stronger than that of a single spike. Bursts have been suggested to cause supralinear summation of EPSPs in pyramidal-pyramidal synapses and pyramidal-interneuron synapses and discharge postsynaptic targets more reliably than the same number of single spikes separated by longer intervals (Csicsvari et al., 1998; Miles and Wong, 1987; Thomson, 2000). Second, bursts in hippocampal pyramidal cells have been implicated in synaptic plasticity. Pairing presynaptic activity with postsynaptic bursts in hippocampal pyramidal cells in vitro results in long-term potentiation of the activated synapses (Magee and Johnston, 1997; Paulsen and Sejnowski, 2000; Pike et al., 1999; Thomas et al., 1998). However, the behavioral, network, and cellular conditions under which a burst will be initiated are not yet clear (Bair et al., 1994; Quirk et al., 2001).

The simplest explanation for the occurrence of bursts is that they are a consequence of large membrane depolarization as a result of strong afferent excitation. Under this scenario, small depolarization levels would mean the cell is silent; moderate depolarization would lead to single spikes; and the largest amount of depolarization would cause the cell to fire in burst mode. Bursts would therefore code for the same stimulus dimension as single spikes but with a greater signal-to-noise ratio (Lisman, 1997; Livingstone et al., 1996). Alternatively, bursting might reflect features other than overall somatic depolarization such as temporal properties of excitatory afferent activity, the effects of inhibitory interneurons (Miles et al., 1996), or an interaction between afferent excitation/inhibition and intrinsic membrane properties. Proper investigation of these issues requires the intact networks and their physiological activation. The main goal of the present experiments was to determine the factors that lead to burst activity in hippocampal pyramidal cells of behaving animals. We find that burst occurrence in the intact brain requires two conditions to be met: a sufficient level of excitation coupled with preceding silence (nonspiking of the neuron).

Results

Variability of Complex Spike Bursts In Vivo

Complex spike bursts of pyramidal cells are considered to be discrete events, distinguished from single spikes by short within-burst interspike intervals (ISI) and decreasing extracellular amplitudes (Kandel and Spencer, 1961; Ranck, 1973). While these qualitative criteria are sufficient to identify typical examples, quantitative identification of burst events is not straightforward. Figure 1A shows examples of a canonical complex spike burst, a single spike, and an intermediate form (“pseudoburst”) consisting of a series of spikes of decreasing amplitude but much larger ISIs (7–20 ms) than typical bursts. The variability of spike amplitude in bursting cells also poses a serious technical challenge to the study of bursting from extracellular data, because smaller amplitude spikes may not be detected or may be misclassified as belonging to a different cell (Harris et al., 2000). To deal with this issue, we devised a quantitative measure of unit isolation quality (see Experimental Procedures). Of the 397 unit clusters that would be judged well isolated by widely used criteria, only 66 met our strict criteria and were analyzed further.

Analysis of the ISI histograms (Figure 1B) revealed a large peak between 2 and 6 ms, corresponding to intraburst ISIs. For larger ISIs, the histogram count continued to decrease exponentially, with no clear gap between intra- and interburst ISIs. This was true for ISI histograms of individual cells and for the pooled ISI histogram of all cells (Figure 1B). For further analysis, we used the commonly adopted criterion, defining a complex spike burst as a series of two or more spikes with ≤ 6 ms intervals (Ranck, 1973). The exact choice of cutoff threshold was not critical; qualitatively similar

¹ Correspondence: buzszaki@axon.rutgers.edu

² These authors contributed equally to this work.

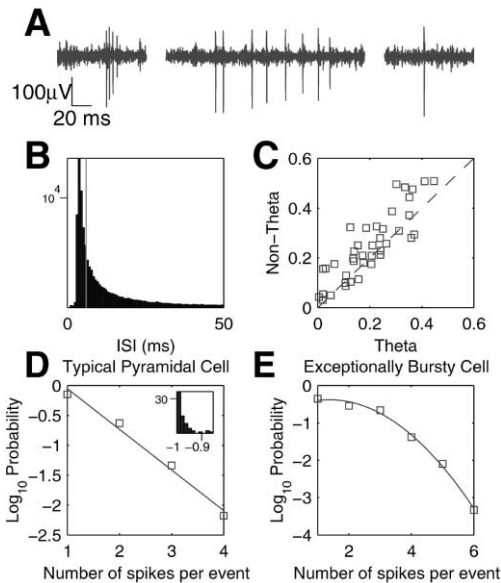


Figure 1. Variability of Complex Spikes In Vivo

(A) A canonical complex spike burst, an intermediate case (pseudoburst), and a single spike.
 (B) Histogram of ISIs for all cells. No clear distinction is visible between intra- and interburst ISIs. Vertical line corresponds to the arbitrary threshold of 6 ms used to define bursting.
 (C) Variability in bursting between cells. Each point represents a cell, with the fraction of ISIs < 6 ms during the theta state on the x axis and during nontheta on the y axis. Burst probability is highly variable and correlated between the two states. In addition, bursting is stronger during nontheta activity.
 (D) Probability distribution of burst lengths for a typical cell. Burst length 1 indicates a single spike. The linear fit indicates an exponential distribution. Inset: linear correlation coefficient for all cells.
 (E) For exceptionally bursty cells, a trend away from the exponential distribution is evident.

results were obtained using ISI thresholds up to ~ 15 ms (see below).

The “burstiness” of neurons, as measured by the fraction of ISIs ≤ 6 ms, varied considerably between cells (Figure 1C). Nevertheless, the burstiness of a given neuron showed stability across different behaviors, as demonstrated by the strong correlation between burstiness during theta and nontheta states. The incidence of complex spike bursts was also, in general, larger during the nontheta state as compared with the theta state (Figure 1C). During theta oscillations, no systematic difference was found in the phase preference of bursts and single spikes.

The number of spikes within a burst varied extensively within bursts of a single neuron as well as between neurons. For the majority of neurons, the probability of seeing n spikes in a burst decreased exponentially with n , as reflected by the linear fit of burst length probability on a logarithmic scale (Figure 1D) (Metzner et al., 1998). In neurons showing long bursts, the burst length distribution was supraexponential (Figure 1E).

Behavioral Correlates of Bursts and Single Spikes

If complex spike bursting is a result of strong dendritic excitation, the proportion of bursts should increase dur-

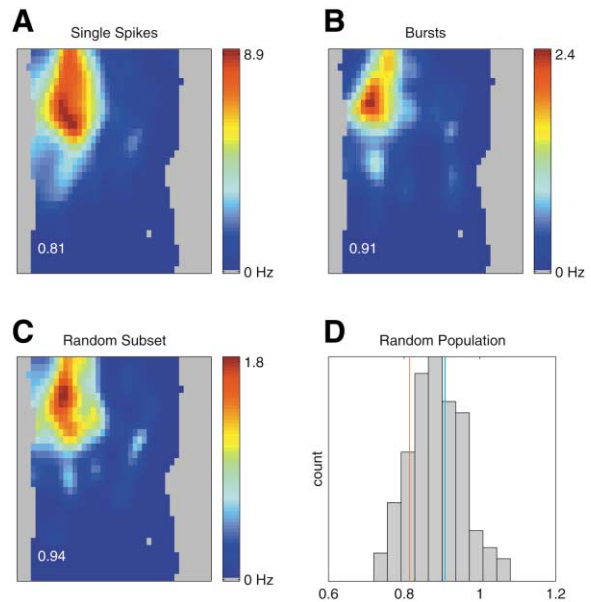


Figure 2. Comparison of Place Fields Constructed from Bursts and Single Spikes

(A) Place field for single spikes of a pyramidal cell.
 (B) Place field for burst events of this cell appears smaller and has a higher sharpness measure.
 (C) To investigate the effects of small-sample bias, a place field was constructed from a random subset of single spikes containing the same number of spikes as there were bursts. This place field also appears visually smaller and has a higher sharpness measure.
 (D) Histogram showing the distribution of the sharpness index for 200 such random subsets. The sharpness measure for single spikes (red) and bursts (blue) do not differ significantly from the random population.

ing periods of high activity. Because hippocampal pyramidal cells fire selectively in restricted regions of space (“place fields”) (O’Keefe and Dostrovsky, 1971), we examined the spatial correlates of burst firing in a pellet chasing task (Muller et al., 1987). If bursting is produced by strong excitation, we reasoned that the ratio of bursts to single spikes would also be spatially modulated, being largest in the place field center where the strongest depolarization is expected. As a result, we expected the place fields constructed from burst events to be sharper than place fields constructed from single spikes, as has been previously suggested (Lisman, 1997; Otto et al., 1991). We set about investigating these previous observations quantitatively using an information-theoretic measure of place field sharpness (Skaggs et al., 1993).

The database did indeed contain some cells for which the place fields constructed from bursts appeared sharper, one of which is shown in Figure 2. This visual impression was quantified by an increase of the place sharpness index from 0.81 (single spikes) to 0.91 (bursts). However, both the subjective impression and information measure are subject to bias due to the smaller number of burst events compared with single spikes. To avoid this bias, we constructed random subsets of the single spikes, with the number of spikes per subset equal to the number of burst events. Figure 2C shows the place field generated by one such random subset. The place field appears sharper, and the infor-

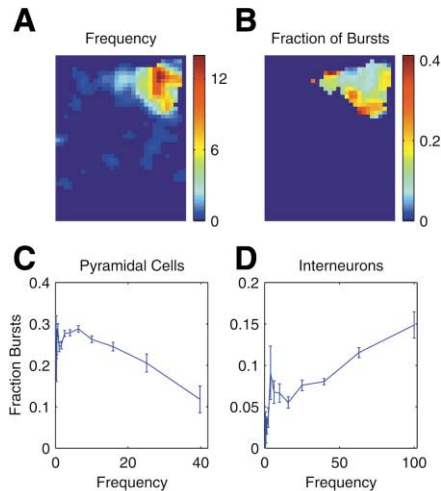


Figure 3. Spatial Dependence of Burst Proportion
(A) Place map for a single pyramidal cell. Color scale: number of events (bursts or single spikes) per second.
(B) Proportion of burst events as a function of position. Burst proportion is highest on the periphery of the place field, but decreases in the center of the place field. No bursts occur far from the field.
(C) Spatial areas of similar frequency were grouped together for all cells and burst proportion computed as a function of frequency (see Experimental Procedures).
(D) Control analysis for interneurons. Burst proportion increases consistently with firing rate.

mation measure is higher than that for all single spikes in this particular example (0.94). Comparison of the “sharpness” for bursts to a population of 200 random subsets of single spikes showed that the burst place field was not significantly sharper than the population of random subsets (Figure 2D). Of 54 well-isolated pyramidal “place” cells recorded during free exploration, burst place fields were significantly sharper in 12 cells and significantly less sharp in 7 cells ($p < 0.05$; 2-tailed quantile test). As a control, we performed the same analysis on interneurons ($n = 26$), which carry less spatial information than pyramidal cells (Muller et al., 1987) and do not fire complex spike bursts (Freund and Buzsáki, 1996). By arbitrarily defining an “interneuron burst” as a set of spikes separated by ≤ 6 ms intervals, the information conveyed per “burst” was significantly larger in 21 interneurons, with no significant effect in the remaining 5.

These findings indicate that, for pyramidal cells, the place fields of bursts are not, in general, sharper than those of single spikes. However, this does not imply that the spatial correlates of bursts and single spikes are identical. To investigate the spatial correlates of bursts in a more direct fashion, we considered the spatial dependence of burst proportion (i.e., the fraction of all neuronal events which are bursts). If the place fields of bursts were the same shape as the place fields of single spikes (i.e., if the firing rate maps were scaled by a constant multiple), burst proportion would be independent of position. Figures 3A and 3B show firing rate and burst proportion as a function of space for a single pyramidal cell. The proportion of bursts was highest, not in the place field center, but rather, in the periphery

of the place field. To determine whether this observation held in general, we computed burst proportion for each bin of a spatial grid and related it to mean event frequency (number of burst or single spike events per second) in that bin. The behavior seen in the example case is borne out at the group level, with the largest proportion of bursts in regions where mean event frequency was 6–7 Hz and lower proportions at higher and lower frequencies (Figure 3C; see Experimental Procedures). In most cells, this occurred at the periphery of the place field. However, in cells with place field center rates in the theta range, the burst proportion was typically highest in the field center. These neurons were the ones for which the place field of bursts was sharper than that of single spikes (see above). As a control, the same relationship was examined for interneurons and for the same pyramidal cells using longer ISI thresholds (pseudobursts). The control analysis of interneurons (Figure 3D) showed an increasing proportion of “bursts” with frequency. Pseudobursts showed similar behavior to that of interneurons (not shown), with the break between burst and pseudoburst behavior occurring at an ISI threshold of ~ 15 ms.

Relationship of Burst Activity to Firing Rate

To further clarify the above observations, we examined the relationship between burst proportion and event frequency independent of the ongoing behavior. According to the depolarization hypothesis, an increased proportion of bursts was expected during periods of strong activity. Contrary to the hypothesis, the proportion of bursts decreased at high event frequencies (Figure 4A). In addition, the proportion of bursts also decreased at the lowest firing rates (< 5 Hz). For the two control cases of pyramidal cell pseudobursts (Figure 4B) and interneuron “bursts” (Figure 4C), however, “burst” proportion showed a consistent increase with firing rate. The breakpoint between burst and pseudoburst behavior was again seen at an ISI threshold of ~ 15 ms. These findings suggested that the conditions that produce maximal firing rates do not necessarily produce a maximal proportion of bursts in pyramidal cells.

Temporal Properties of Burst Firing

The results above suggest that pyramidal cell bursting is not a simple reflection of increased afferent excitation. To investigate the conditions that may be controlling burst activity, we examined the temporal properties of the spike train in more detail. Figure 5A illustrates a “return map” for a single neuron, which shows the relationship between each successive pair of ISIs. The solid line shows the running median of ISI as a function of the preceding ISI. The median ISI is small when preceded by short ISIs, reaches a maximum when preceded by ISIs of ~ 10 ms, and becomes small again for long preceding ISIs (10^2 – 10^3 ms). To express these features more explicitly, the probability of burst length ISIs (≤ 6 ms) is plotted as a function of previous ISI in Figure 5B. Short ISIs had a high probability of being followed by a second short ISI, corresponding to bursts of three or more spikes. For longer ISIs, burst probability increases steadily with ISI, ranging from 0.1 to 0.8. If the graph was replotted using only spikes from theta or nontheta epochs, it ap-

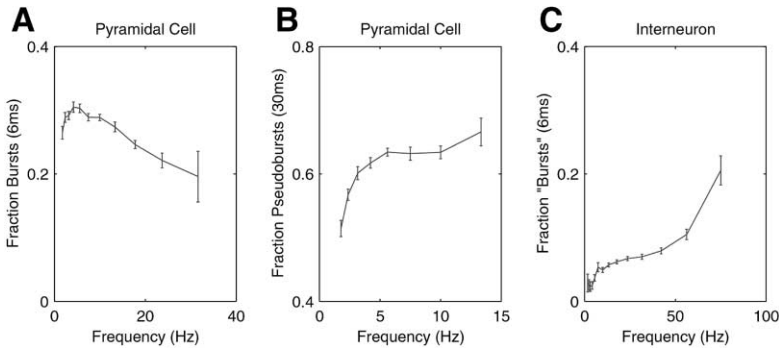


Figure 4. Dependence of Burst Proportion on Event Frequency

Spike trains during awake and sleep behavior were divided into 2 s bins. For each cell, bins of similar frequency were grouped together, and the fraction of bursts computed for each group (see Experimental Procedures).

(A) Burst proportion as a function of event frequency, averaged over all cells. Note the peak at approximately 6 Hz.

(B) Control case of pseudobursts, defined to be series of spikes separated by at most 30 ms. Burst proportion increases monotonically with event frequency.

(C) Control case of interneuron "bursts." Again, a monotonic increase is seen.

peared similar (data not shown). There was also a small but significant increase in burst probability in nontheta over theta after ISIs of up to ~ 50 ms. These results showed that burst initiation was most probable after a period of nonspiking activity in both theta and nontheta states.

To quantify the temporal dynamics at the group level, the ratio of burst initiation probability after long ISIs (10^2 – 10^3 ms) and intermediate ISIs (10^1 – 10^2 ms) was calculated for each pyramidal neuron. To ensure accurate estimation of the ratio, only cells that fired ≥ 10 spikes in both conditions were used. Of the 57 such cells, the ratio exceeded unity in 51, indicating that the probability of bursting in pyramidal cells is significantly higher after a period of silence than after recent spiking ($p < 0.0001$; sign test).

This conclusion is further illustrated by comparing the distribution of activity occurring before and after single spikes and bursts of various lengths in the example cell

(Figure 5C). For single spikes, little difference was seen between activity before and after the spike. In contrast, complex spike bursts tended to be preceded by periods of low activity. Across the population, the median ISI preceding single spikes was 48 ms. The median ISIs preceding bursts of length 2, 3, 4, and ≥ 5 were 119, 260, 371, and 480 ms (Figure 6A), displaying a strongly significant increase with burst length ($p < 0.0001$, Kruskal-Wallis test)

The above analysis has indicated that bursting is suppressed by prior activity. Are bursts in particular more effective than single spikes in reducing the probability of subsequent burst initiation? To address this question, we plotted the probability of burst initiation as a function of the time since the previous event and the nature of the previous event (Figure 6B). Single spikes and bursts were equally effective at suppressing subsequent burst initiation. We therefore conclude that the effect of bursting on subsequent activity is not different from the effect of single spikes. Notice also that after very long intervals (1–10 s), the probability of burst decreases again, a finding which may be compared to the lower fraction of bursts at times or places of very low firing rates.

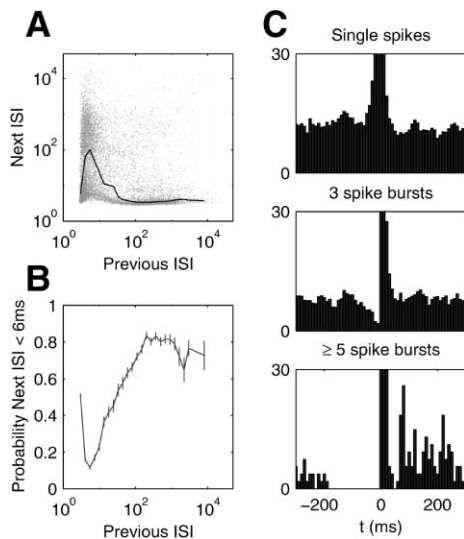


Figure 5. Spike Dynamics for an Example Cell

(A) Return map of ISIs. Each dot represents a pair of consecutive ISIs. The black line indicates a running median.

(B) Probability that an ISI is less than 6 ms, as a function of the preceding ISI.

(C) Averaged spike frequency, aligned on the first spike of bursts of various lengths. Silent periods occur before bursts, with longer silences before longer bursts.

Spike Amplitude Predicts Burst Probability

Because extracellular spike amplitude also shows a dependence on recent firing history (Quirk and Wilson, 1999), we examined whether spike amplitude and burst initiation probability might be related. Figure 7A illustrates the variability of extracellular spike amplitude for a typical pyramidal cell. The amplitude of extracellular spikes was particularly variable during place field traversals, corresponding to the vertical "bands" of dots. The fine structure of these bands demonstrated three noticeable features (Figure 7B). First, there was a general downward trend in amplitude throughout the firing period (Quirk et al., 2001). Second, spikes following a long ISI (shown in blue) tended to initiate bursts, but those following shorter ISIs did not. Third, spikes that initiated bursts tended to have larger amplitudes than isolated single spikes.

The data so far have shown that burst probability and spike amplitude are both correlated with previous ISI. We therefore expect that burst probability will also be correlated with spike amplitude. Mean wideband waveforms of single spikes and spikes initiating bursts of varying lengths are shown in Figure 7C for an example

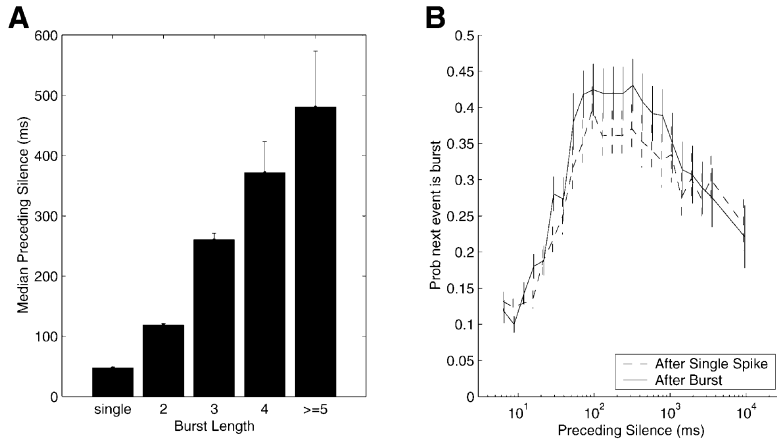


Figure 6. Spike Dynamics at the Group Level (A) Median length of the preceding silent period as a function of burst length. A consistent increase is seen.

(B) The probability that an event will be a burst, as a function of the length of silence preceding it, averaged over all cells. The probability increases with length of silence but decreases again for very long silent periods (1–10 s). The data are separated according to whether the previous event was a single spike or a burst; there is little difference between the two.

cell. The effect of spike amplitude on burst probability was confirmed at the group level with logistic regression ($t = 75.7$; $p < 0.0001$; data from different cells were pooled after standardization of amplitude to the same mean and variance). However, the question remains whether burst probability and amplitude are *partially*

correlated, i.e., whether the correlation persists after the common effect of ISI is accounted for. Figure 7D shows the relationship between preceding ISI, amplitude, and burst initiation for an example cell. It can be seen that spike amplitude is larger for burst first spikes than for single spikes, even after a fixed preceding ISI. This effect

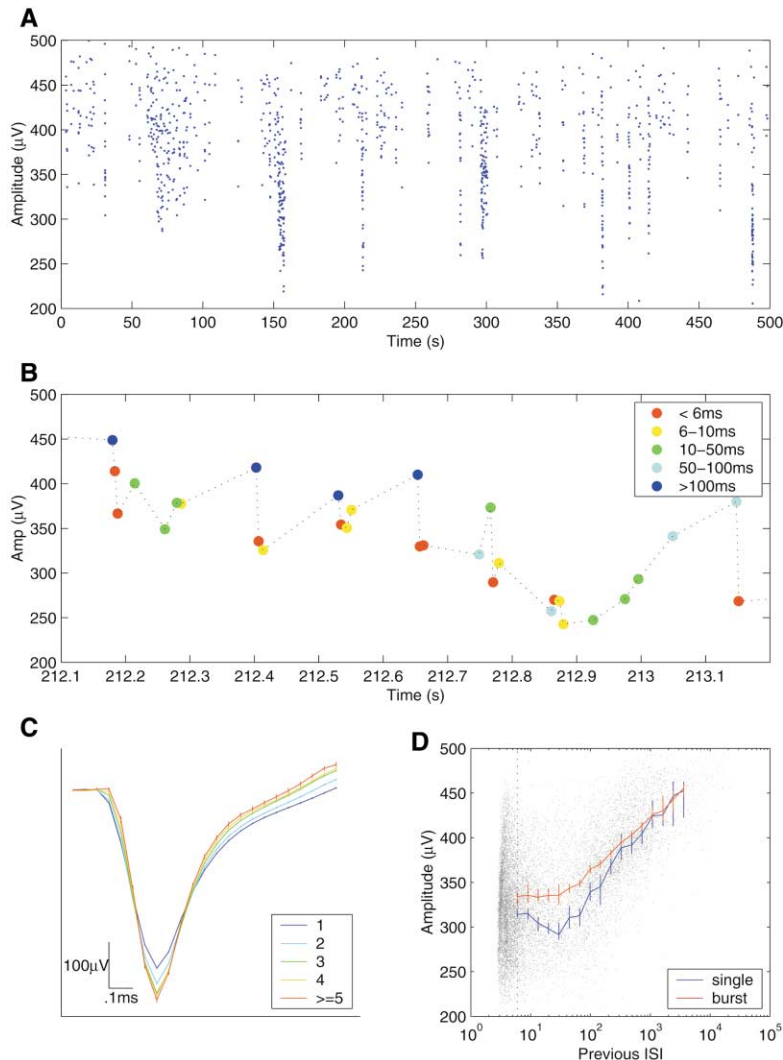


Figure 7. Bursts Are Initiated Preferentially by Spikes of Large Extracellular Amplitude

(A) Extracellular spike amplitude versus time. Each dot represents a spike. The vertical bands correspond to periods of increased firing rate caused by place field traversals, characterized by increased variability in extracellular amplitude.

(B) A single place-field traversal. Each dot corresponds to an action potential and is color coded according to preceding ISI length (see legend).

(C) Mean waveforms for single spikes and first spikes of bursts of various lengths for the above cell. Longer bursts are initiated by larger amplitude, narrower spikes. Error bars show SEM.

(D) Relationship between amplitude, preceding ISI, and burst induction. Gray points: scatter plot of extracellular amplitude versus preceding ISI. The blue and red lines show running median amplitude as a function of ISI for single spikes and burst first spikes. Burst initiating spikes are larger in amplitude, even for the same preceding ISI.

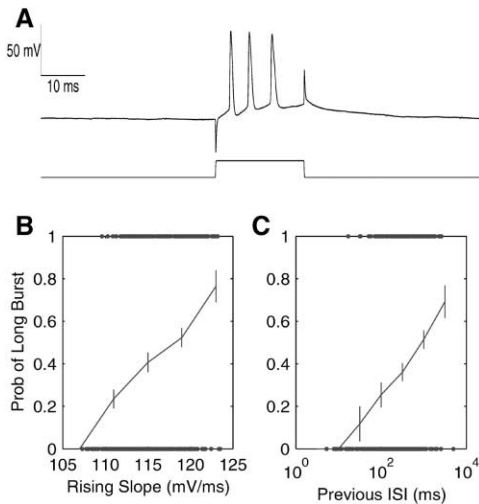


Figure 8. Relation of Burst Probability to Intracellular Rising Slope
Intracellular current step injections (20 ms steps of 0.65 nA, every 3 s), produced bursts of varying length (typically 3 or 4 spikes) in a pyramidal cell.

In between current steps, the cell fired sporadic single spikes. Bursts were divided into “long” and “short” according to whether the number of spikes in the burst was greater or less than mean.

(A) Example data segment showing a step-induced burst.

(B) Burst length was correlated with the intracellular rising slope of the initial action potential.

(C) Burst length was correlated with the length of the preceding silent period.

was confirmed at the group level with partial logistic regression ($t = 51.7$, $p < 0.0001$). Burst length was also correlated with the extracellular amplitude of the initiating spike at the group level, with bursts of length 2, 3, 4, and ≥ 5 being initiated by spikes of amplitude 5%, 10%, 13%, and 18% above mean single spike amplitude ($p < 0.0001$, Kruskal-Wallis test).

Intracellular Correlates of Burst Length

The data in the behaving rat indicated that the probability of burst initiation is correlated with extracellular spike amplitude. Previous work has shown that the extracellular spike waveform is well approximated by the first derivative of the intracellular action potential during the rising phase (Henze et al., 2000; Jack et al., 1975). We therefore examined the relationship between burst length and intracellular action potential rising slope directly in five cells in intact anaesthetized rats. Burst discharges were evoked by the standard method of injecting sufficiently strong somatic current steps (0.5–1 nA, 20–25 ms), which caused bursts of 2–5 spikes (Figure 8A). This method has the advantage that the parsing of a spike train into single spikes and bursts is clear. However, caution is in order since somatic current injection bursts may have different properties compared to those that occur naturally *in vivo*.

For each cell, the rate of rise of the first action potential was positively correlated with the numbers of spikes within the burst (logistic regression; $p < 0.01$ for each cell) (Figure 8B). In addition, we examined the effect of spontaneously occurring spikes on the current step-induced burst duration. Similar to the observations in

the behaving rat, burst probability was correlated with the time since the last spike ($p < 0.01$ for each cell) (Figure 8C). Because the induced bursts occurred independent of the network activity, these intracellular experiments also support the hypothesis that the temporal relationship between single spikes and burst is the critical variable for burst length rather than some undetected coordinated network event.

Discussion

The main findings of the present experiments are that for CA1 pyramidal cells: (1) bursting did not in general occur preferentially in place field centers, but rather, in regions of space where the neurons discharged at intermediate frequencies (6–7 Hz); (2) the probability of burst initiation is largest after sustained (100 ms–1 s) periods of neuronal silence; and (3) the probability and length of the burst are correlated with extracellular spike amplitude and intracellular action potential rising slope.

Conditions for Generation of Complex Spike Bursts

The fraction of complex spikes was larger after extended periods of neuronal silence (100 ms–1 s) than after short intervals. Furthermore, the number of spikes within a burst correlated with the length of the preceding silent period. However, in locations far from the place field center where the overall firing rate was low, or after very long silent periods (>1 s), the fraction of complex spikes was reduced. We therefore suggest that burst production reflects an interplay of two factors: stronger depolarization increases burst probability, but it is counterbalanced by a suppression of bursting by recent activity. The ideal condition for producing a burst would therefore be a period of silence followed by strong dendritic excitation. Strong but tonic excitation would cause a smaller proportion of bursts, as it would lead to firing of prior spikes, and there would not be a sufficient silent period.

We propose that complex spike bursts can be conceived as conditional synchrony detectors, occurring when two criteria are met: strong synchrony of excitatory afferents and a preceding prolonged silent period. According to this reasoning, during periods of sustained activity, strong synaptic excitation will elicit further single spikes, but after a period of inactivity, the same afferent input is more likely to induce a complex spike burst. Further support for this proposal is that weak commissural stimulation of CA1 pyramidal cells causes an initial suppression of unit firing, followed by a rebound period when bursts are observed (Buzsáki and Czeh, 1981). The tendency of pyramidal cells to produce bursts after silent periods may be thought of as complementary to firing rate adaptation; bursting serves to enhance the neuron’s response at the onset of a period of excitation, while adaptation serves to diminish its response to continuing excitation.

While our findings were derived from recordings of hippocampal pyramidal cells, the temporal dynamics described here may also apply to bursting cells elsewhere in the nervous system. It is notable that return maps of thalamocortical neurons show very similar dy-

namics to the present observations in CA1 pyramidal cells (Reinagel et al., 1999). Furthermore, in visual cortex, bursts tend to occur after microsaccades, when cells undergo a sudden excitation after a period of silence (Martinez-Conde et al., 2000).

Possible Mechanisms of Activity-Dependent Burst Suppression

What mechanisms might underlie the suppression of bursting by recent activity? The correlation of burst probability and length with extracellular amplitude suggests that burst suppression may result from activity-dependent modulation of some cellular variable, which is reflected in the extracellular amplitude.

The classical model of complex spike burst generation assumes that burst firing is generated by activation of dendritic Ca^{2+} and/or Na^+ currents subsequent to somadendritic back propagation of the action potential (Andreasen and Lambert, 1995; Azouz et al., 1996; Pinsky and Rinzel, 1994; Su et al., 2001; Traub et al., 1994; Wong and Prince, 1981). We therefore consider whether the suppression effect may be understood by assuming that burst initiation probability is a function of the magnitude of somadendritic back propagation. The temporal dynamics of burst probability and spike back propagation are similar, with suppression by previous spiking activity and a recovery period in the hundreds of milliseconds (Spruston et al., 1995; Jung et al., 1997; Mickus et al., 1999). The main cause of the decrease in back propagation is prolonged Na^+ channel inactivation. We suggest that prolonged Na^+ channel inactivation may account for the suppressing effects of previous spikes and that the availability of Na^+ channels determines burst initiation and duration. Supporting this suggestion, burst length in the intracellular preparation was correlated with the rising slope of the intracellular action potential, which reflects the speed of Na^+ entry and, therefore, the activation status of Na^+ channels. Furthermore, burst initiation probability and length were correlated with extracellular amplitude, which reflects the magnitude of current flow during the action potential rising phase (Henze et al., 2000; Jack et al., 1975). In this context, network effects might also play a role in the control of burst firing. For example, strong inhibition following a period of activity could deinactivate Na^+ channels and, thus, facilitate burst occurrence.

The increased burst probability during nontheta over theta may also be explained by this mechanism. In theta, most spikes occur during brief epochs of rapid firing corresponding to place field traversals. Therefore, greater Na^+ channel inactivation is expected compared with the nontheta state where such intense firing periods do not occur. Evidence for cumulative inactivation during a place field traversal may be seen in the slow decrease in amplitude as the rat crosses the field (Figure 7B) (Quirk et al., 2001).

Other cellular mechanisms may also contribute to the activity-dependent suppression of bursts. One possibility is Ca^{2+} -dependent K^+ channels (Traub et al., 1994). However, this mechanism may not fully explain our results. If Ca^{2+} -dependent channels mediate burst suppression, then bursts should cause more suppression than single spikes (because bursts cause more Ca^{2+}

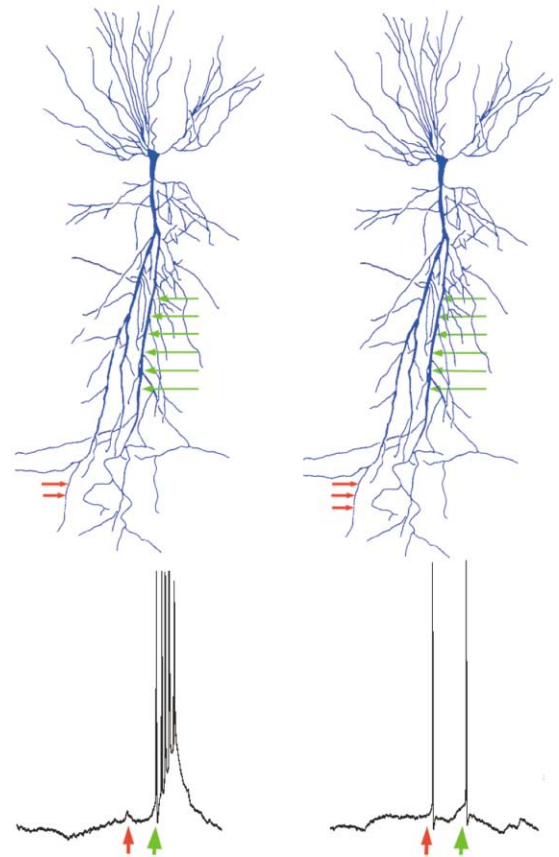


Figure 9. Hypothesized Effect of Activity-Dependent Burst Suppression on Synaptic Plasticity

A weak input (red) is followed by a strong input (green). If the weak input is subthreshold (left), the strong input can trigger a burst and can lead to strengthening of the weak input. If the weak input is suprathreshold (right), the evoked single spike can inhibit burst response to the same strong input. In effect, the firing of already potentiated afferents reduces the efficacy of the strong input and inhibits further potentiation.

influx). However, the relationship of bursts to subsequent activity was not different from that of single spikes.

Functional Implications

The finding that the proportion of bursts is largest for event rates of 6–7 Hz suggests that there is a point at which the balance between excitation and suppression by preceding activity leads to maximum burst probability. Interestingly, this balance point occurs for firing rates equal to the frequency of the hippocampal theta rhythm. Theta modulated inhibition (Freund and Buzsáki, 1996) may provide the silences and/or deinactivation necessary to produce rhythmic bursting. Bursts of spikes at theta frequency have been shown to be particularly efficacious for inducing LTP in hippocampal pyramidal cells (Huerta and Lisman, 1993; Larson and Lynch, 1986; Otto et al., 1991). Our data suggest that cellular mechanisms may be tuned to produce precisely this kind of activity.

The computational function of bursts is often considered in terms of the effect on postsynaptic cells (Lisman,

1997; Thomson, 2000). However, *in vitro* evidence suggests that bursts may also play a critical role in modifying synaptic efficacy in the bursting cell, with the occurrence of a weak (subthreshold) input prior to a strong, burst-inducing input leading to strengthening of the weak synapse (Magee and Johnston, 1997; Pike et al., 1999; Thomas et al., 1998). The closer the weak and strong inputs are in time, the stronger the ensuing synaptic modification (Bi and Poo, 1998; Markram et al., 1997; Magee and Johnston, 1997). It is interesting to speculate on the possible effects of the interplay between the single spike and burst activity described here on this type of synaptic plasticity (Figure 9). If the weak input is subthreshold, the strong input will cause a burst, and the weak pathway will be strengthened. However, if the weak input is large enough to initiate a spike, this spike may inhibit the later occurrence of the burst and consequent synaptic modification. The closer the weak (but suprathreshold) and strong inputs are in time, the stronger the veto effect of the single spike. Our findings suggest that the firing mode of pyramidal cells is determined by a subtle interplay of the intrinsic properties of neurons and the timing of afferent neuronal networks. Furthermore, this interplay may affect the conditions for synaptic plasticity in the intact brain.

Experimental Procedures

Physiological Methods

Eighteen male rats of the Long-Evans strain (300–500 g) were implanted with tetrodes. Prior to implantation, seven rats were trained to run continuously in a running wheel for water reinforcement available in an adjacent box (Czurko et al., 1999). The remaining 11 animals were recorded while exploring in a large rectangular box (1.2 m X 1.2 m, 0.5 min high). An infrared LED was attached to the head stage to track the position of the animal. The location of all tetrodes was histologically confirmed to be the CA1 pyramidal layer.

After amplification and band-pass filtering (1 Hz–5 kHz), field potentials and extracellular action potentials, together with the behavioral events, were digitized continuously at 20 kHz with a DataMax system (16-bit resolution; RC Electronics, Santa Barbara, CA). All experimental procedures were in accordance with Rutgers University guidelines.

Data Analysis

Extracellular spikes were extracted from the traces by previously described methods (Csicsvari et al., 1998). For each spike, a 12-dimensional feature vector was calculated by computing three principal components for each channel. Units were separated by automatic cluster analysis followed by manual adjustment (Harris et al., 2000). In order to ensure that only well-isolated units were included in the analysis, we defined a measure of unit isolation, termed “isolation distance.” It is defined to be the Mahalanobis distance from the identified cluster within which as many spikes belong to the specified cluster as to others. This measure estimates the distance from this cluster to the nearest other cluster. We only considered units with isolation distances >50.

Theta activity was detected by calculating the ratio of the Fourier components of the theta (5–10 Hz) and delta (2–4 Hz) frequency bands. A ratio of >6 identified theta epochs, and a ratio of <3 identified non theta epochs (Csicsvari et al., 1998).

Calculation of Place Fields

Place fields were calculated using a kernel-based method. The firing rate at a point x was estimated by

$$f(x)dt = \frac{\sum_i n_i w(|x - x_i|)}{\sum_i w(|x - x_i|)}$$

Here, n_i is the number of spikes fired in a given time bin, x_i is the position of the rat in that time bin, and dt is the time bin size. The kernel function w was a Gaussian of width 3 cm.

Quantification of Place Field Sharpness

Place field sharpness was quantified using a previously described information-theoretic measure (Skaggs et al., 1993). This measures the specificity of cell firing by quantifying the amount of information in the spike train about the position of the rat, measured in bits per spike. It is calculated as

$$I = \sum_x \frac{\lambda(x)}{\lambda} \log_2 \frac{\lambda(x)}{\lambda} p(x) dx,$$

where x is spatial location, $p(x)$ is the probability density for the rat being at location x , $\lambda(x)$ is the firing rate at location x , and λ is the overall mean firing rate. More spatially specific firing leads to a larger value of this measure. With information-theoretic measures, one must beware of small-sample bias, dependent on the total number of spikes and estimation parameters (in this case the smoothing width). A randomization method was therefore used, comparing the spatial specificity of burst events to the spatial specificity of random subsets of the single spikes, with the size of the random set being the same as the number of burst events.

Relationship of Burst Probability to Frequency

For each unit, spike activity was classified into bursts (series of two or more spikes separated by no more than 6 ms) and single spikes. Single cell spike trains were binned either by time (into overlapping 2 s windows) or by space (according to the rat's position on a 21 × 16 grid). For each bin, the number of events (bursts or single spikes) was computed. Bins with ≤ 2 events were excluded. Bins of similar event frequency (number of events divided by total time in the bin) were grouped together according to the smallest integer greater than or equal to $8\log(f)$ (a log scale was used to compensate for the smaller number of bins of high frequency). For each frequency, the burst proportion was calculated as the total number of bursts divided by the total number of events for all bins of that frequency. For each frequency, burst proportion was averaged across cells. Error bars were estimated by a repeated measures procedure as the standard error of burst proportion across cells after subtracting overall means for each cell.

Intracellular Recording In Vivo

Intracellular *in vivo* recordings were obtained in urethane-anaesthetized rats, as described previously (Henze and Buzsáki, 2001). Bursts of 2–5 spikes were induced by injection of depolarizing current steps (0.5–1 nA, 20–25 ms) at regular intervals (3–5 s).

Acknowledgments

This work was supported by NIH (NS34994, MH54671 to G.B., MH12403 to D.A.H.), F.M. Kirby Foundation, Human Frontier Science Program (X.L.), and the Uehara Memorial Foundation (H.H.).

Received February 5, 2001; revised July 6, 2001.

References

- Andreasen, M. and Lambert, J.D. (1995). Regenerative properties of pyramidal cell dendrites in area CA1 of the rat hippocampus. *J. Physiol. (Lond)* **483** (Pt 2), 421–441.
- Azouz, R., Jensen, M.S., and Yaari, Y. (1996). Ionic basis of spike after-depolarization and burst generation in adult rat hippocampal CA1 pyramidal cells. *J. Physiol.* **492**, 211–223.
- Bair, W., Koch, C., Newsome, W., and Britten, K. (1994). Power spectrum analysis of bursting cells in area MT in the behaving monkey. *J. Neurosci.* **14**, 2870–2892.
- Bi, G.Q., and Poo, M.M. (1998). Synaptic modifications in cultured hippocampal neurons: dependence on spike timing, synaptic strength, and postsynaptic cell type. *J. Neurosci.* **18**, 10464–10472.
- Buzsáki, G., and Czeh, G. (1981). Commissural and perforant path

- interactions in the rat hippocampus. Field potentials and unitary activity. *Exp. Brain Res.* **43**, 429–438.
- Connors, B.W., Gutnick, M.J., and Prince, D.A. (1982). Electrophysiological properties of neocortical neurons in vitro. *J. Neurophysiol.* **48**, 1302–1320.
- Csicsvari, J., Hirase, H., Czurko, A., and Buzsáki, G. (1998). Reliability and state dependence of pyramidal cell-interneuron synapses in the hippocampus: an ensemble approach in the behaving rat. *Neuron* **21**, 179–189.
- Czurko, A., Hirase, H., Csicsvari, J., and Buzsáki, G. (1999). Sustained activation of hippocampal pyramidal cells by 'space clamping' in a running wheel. *Eur. J. Neurosci.* **11**, 344–352.
- Freund, T.F., and Buzsáki, G. (1996). Interneurons of the hippocampus. *Hippocampus* **6**, 347–470.
- Gray, C.M., and McCormick, D.A. (1996). Chattering cells: superficial pyramidal neurons contributing to the generation of synchronous oscillations in the visual cortex. *Science* **274**, 109–113.
- Harris, K.D., Henze, D.A., Csicsvari, J., Hirase, H., and Buzsáki, G. (2000). Accuracy of tetrode spike separation as determined by simultaneous intracellular and extracellular measurements. *J. Neurophysiol.* **84**, 401–414.
- Henze, D.A., Borhegyi, Z., Csicsvari, J., Mamiya, A., Harris, K.D., and Buzsáki, G. (2000). Intracellular features predicted by extracellular recordings in the hippocampus in vivo. *J. Neurophysiol.* **84**, 390–400.
- Henze, D.A., and Buzsáki, G. (2001). Action potential threshold of hippocampal pyramidal cells in vivo is increased by recent spiking activity. *Neuroscience*, in press.
- Huerta, P.T., and Lisman, J.E. (1993). Heightened synaptic plasticity of hippocampal CA1 neurons during a cholinergically induced rhythmic state. *Nature* **364**, 723–725.
- Jack, J.J.B., Noble, D., and Tsien, R.W. (1975). *Electric current flow in excitable cells.* (Oxford: Clarendon Press).
- Jung, H.Y., Mickus, T., and Spruston, N. (1997). Prolonged sodium channel inactivation contributes to dendritic action potential attenuation in hippocampal pyramidal neurons. *J. Neurosci.* **17**, 6639–6646.
- Kandel, E.R., and Spencer, W.A. (1961). Electrophysiology of hippocampal neurons. II. Afterpotentials and repetitive firing. *J. Neurophysiol.* **24**, 243–259.
- Larson, J., and Lynch, G. (1986). Induction of synaptic potentiation in hippocampus by patterned stimulation involves two events. *Science* **232**, 985–988.
- Lisman, J.E. (1997). Bursts as a unit of neural information: making unreliable synapses reliable. *Trends Neurosci.* **20**, 38–43.
- Livingstone, M.S., Freeman, D.C., and Hubel, D.H. (1996). Visual responses in V1 of freely viewing monkeys. *Cold Spring Harb. Symp. Quant. Biol.* **61**, 27–37.
- Llinas, R., and Jahnsen, H. (1982). Electrophysiology of mammalian thalamic neurones in vitro. *Nature* **297**, 406–408.
- Magee, J.C., and Johnston, D. (1997). A synaptically controlled, associative signal for Hebbian plasticity in hippocampal neurons. *Science* **275**, 209–213.
- Markram, H., Lubke, J., Frotscher, M., and Sakmann, B. (1997). Regulation of synaptic efficacy by coincidence of postsynaptic APs and EPSPs. *Science* **275**, 213–215.
- Martinez-Conde, S., Macknik, S.L., and Hubel, D.H. (2000). Microsaccadic eye movements and firing of single cells in the striate cortex of macaque monkeys. *Nat. Neurosci.* **3**, 251–258.
- Metzner, W., Koch, C., Wessel, R., and Gabbiani, F. (1998). Feature extraction by burst-like spike patterns in multiple sensory maps. *J. Neurosci.* **18**, 2283–2300.
- Mickus, T., Jung, H.Y., and Spruston, N. (1999). Slow sodium channel inactivation in CA1 pyramidal cells. *Ann. NY Acad. Sci.* **868**, 97–101.
- Miles, R., Toth, K., Gulyas, A.L., Hajos, N., and Freund, T.F. (1996). Differences between somatic and dendritic inhibition in the hippocampus. *Neuron* **16**, 815–823.
- Miles, R., and Wong, R.K. (1987). Inhibitory control of local excitatory circuits in the guinea-pig hippocampus. *J. Physiol.* **388**, 611–629.
- Muller, R.U., Kubie, J.L., and Ranck, J.B., Jr. (1987). Spatial firing patterns of hippocampal complex spike cells in a fixed environment. *J. Neurosci.* **7**, 1935–1950.
- O'Keefe, J., and Dostrovsky, J. (1971). The hippocampus as a spatial map. Preliminary evidence from unit activity in the freely-moving rat. *Brain Res.* **34**, 171–175.
- Otto, T., Eichenbaum, H., Wiener, S.I., and Wible, C.G. (1991). Learning-related patterns of CA1 spike trains parallel stimulation parameters optimal for inducing hippocampal long-term potentiation. *Hippocampus* **1**, 181–192.
- Paulsen, O., and Sejnowski, T.J. (2000). Natural patterns of activity and long-term synaptic plasticity. *Curr. Opin. Neurobiol.* **10**, 172–179.
- Pike, F.G., Meredith, R.M., Olding, A.W., and Paulsen, O. (1999). Rapid report: postsynaptic bursting is essential for 'Hebbian' induction of associative long-term potentiation at excitatory synapses in rat hippocampus. *J. Physiol. (Lond)* **518** (Pt 2), 571–576.
- Pinsky, P.F., and Rinzel, J. (1994). Intrinsic and network rhythmogenesis in a reduced Traub model for CA3 neurons. *J. Comput. Neurosci.* **1**, 39–60.
- Quirk, M.C., Blum, K.I., and Wilson, M.A. (2001). Experience-Dependent Changes in Extracellular Spike Amplitude May Reflect Regulation of Dendritic Action Potential Back-Propagation in Rat Hippocampal Pyramidal Cells. *J. Neurosci.* **21**, 240–248.
- Quirk, M.C., and Wilson, M.A. (1999). Interaction between spike waveform classification and temporal sequence detection. *J. Neurosci. Methods* **94**, 41–52.
- Ranck, J.B.J. (1973). Studies on single neurons in dorsal hippocampal formation and septum in unrestrained rats. I. Behavioral correlates and firing repertoires. *Exp. Neurol.* **41**, 461–531.
- Reinagel, P., Godwin, D., Sherman, S.M., and Koch, C. (1999). Encoding of visual information by LGN bursts. *J. Neurophysiol.* **81**, 2558–2569.
- Skaggs, W.E., McNaughton, B.L., Gothard, K.M., and Markus, E. (1993). An information-theoretic approach to deciphering the neural code. In *Advances in Neural Information Processing Systems*, Vol. 5, S. Hanson, J. Cowan, and G. Giles, eds. (San Mateo: Morgan Kaufmann), pp. 1030–1037.
- Spruston, N., Schiller, Y., Stuart, G., and Sakmann, B. (1995). Activity-dependent action potential invasion and calcium influx into hippocampal CA1 dendrites. *Science* **268**, 297–300.
- Su, H., Alroy, G., Kirson, E.D., and Yaari, Y. (2001). Extracellular calcium modulates persistent sodium current-dependent burst-firing in hippocampal pyramidal neurons. *J. Neurosci.* **21**, 4173–4182.
- Thach, W.T. (1968). Discharge of Purkinje and cerebellar nuclear neurons during rapidly alternating arm movements in the monkey. *J. Neurophysiol.* **31**, 785–797.
- Thomas, M.J., Watabe, A.M., Moody, T.D., Makhinson, M., and O'Dell, T.J. (1998). Postsynaptic complex spike bursting enables the induction of LTP by theta frequency synaptic stimulation. *J. Neurosci.* **18**, 7118–7126.
- Thomson, A.M. (2000). Facilitation, augmentation and potentiation at central synapses. *Trends Neurosci.* **23**, 305–312.
- Traub, R.D., Jefferys, J.G., Miles, R., Whittington, M.A., and Toth, K. (1994). A branching dendritic model of a rodent CA3 pyramidal neurone. *J. Physiol.* **481**, 79–95.
- Wong, R.K., and Prince, D.A. (1981). Afterpotential generation in hippocampal pyramidal cells. *J. Neurophysiol.* **45**, 86–97.